UDC 654.165

CAPACITY AND WEIGHT COEFFICIENTS IN MIMO WIRELESS COMMUNICATION CHANNELS BASED ON ADAPTIVE MULTI-BEAM ANTENNAS IN URBAN ENVIRONMENT WITH FADING

N. Blaunstein[a]***,*** *Dr. Sc., Phys.-Math., Professor, nathan.blaunstein@hotmail.com*
Ch. Cristodoulou[b]***,*** *PhD, Professor, christos@ece.unm.edu*
M. B. Sergeev [c]***,*** *Dr. Sc., Tech., Professor, mbse@mail.ru*
[a]*Ben-Gurion University of the Negev, POB 653, 1, Ben Gurion St., Beer Sheva, 74105, Israel*
[b]*University of New Mexico, Albuquerque, NM 87131, USA*
[c]*Saint-Petersburg State University of Aerospace Instrumentation, 67, B. Morskaia St., 190000, Saint-Petersburg, Russian Federation*

Purpose: *Long-Term Evolution (LTE) system has had as many as 12 implementations, the later ones using multi-beam adaptive antennas. LTE development and usage have demonstrated that such systems cannot be adapted to environmental changes, to different locations of every subscriber in the service areas, either open or close for connection, or to the acknowledgement from every wireless channel of a Multiple Input Multiple Output (MIMO) system which goes through an environment with different fading of signals along every individual channel — especially with the permanent need to increase the connection channel capacity and minimize the errors when sending information via time-varying fading channels. As we still lack a general model fully reflecting the fading in every individual wireless channel of a MIMO system, the problem is to connect the signal fading determined by Ricean K-factor with the parameters of an individual channel: its capacity, spectral efficiency and errors in transmitting the information flow.* ***Methods:*** *In order to minimize the effects of fading which is the source of multiplicative noise in every individual MIMO chanel, a mathematical model was developed based on the well-known and experimentally tested model of radiowave propagation in various urban and suburban areas. The Ricean K-factor was found via the known parameters of the environment: building density and profile, distances between the antennas, etc. Then, using the Ricean K-factor, a modification of Shannon's postulate was obtained, which takes into account not only the Gaussian noise but the multiplicative noise, too.* ***Results:*** *For the first time analytical expressions were obtained which connect the weight coefficients used in multi-beam adaptive antenna theory with the parameters of urban environment. The behaviour of Ricean K-factor was described in various suburban and urban environments. This helped to analize the capacity and spectral efficiency of urban channels depending on their fading level and structure of the surrounding buildings. Then, in order to maximize the capacity and spectral efficiency of the MIMO wireless channels, taking into account the direct connection between the fading parameter K and the weight coefficient of a multi-beam antenna, it was analyzed whether it is possible to efficiently connect non-correlated and correlated elements of MIMO antennas.* ***Practical relevance:*** *It was shown for the first time how the weight coefficients of MIMO antenna elements change in an azimuthal plane. This helps to predict the quality of wireless connection for every subscriber located at various angles and various distances from a MIMO antenna system, under various conditions of transceiving the signals along channels with fading.*

Keywords *— Multiple Input Multiple Output, Multi-Beam Antenna, Ricean K-Factor, Capacity, Spectral Efficiency, Weight Coefficients of Antenna Elements.*

Introduction into the MIMO Channels with Fading

Multipath is the propagation phenomenon that results in radio signals reaching the receiving antenna by two or more paths. In terrestrial environments, this phenomenon is caused by reflection, diffraction and scattering from terrestrial objects, such as mountains, lakes, trees, and buildings [1–12] (Fig. 1).

The effects of multipath include constructive and destructive interference, and phase shifting of the signal. As well-known from the literature, *K*-factor of Rician distribution is usually used for the fading and for multiplicative noise description [1–15]. Destructive interference causes fading, when the magnitudes of the signals, arriving by the various paths, have a stochastic nature described by the well-known Rayleigh distribution for the worst NLOS (Non-Line-of-Sight) cases of wireless communication, known as Rayleigh fading, or by Ricean distribution for the channels with exis-

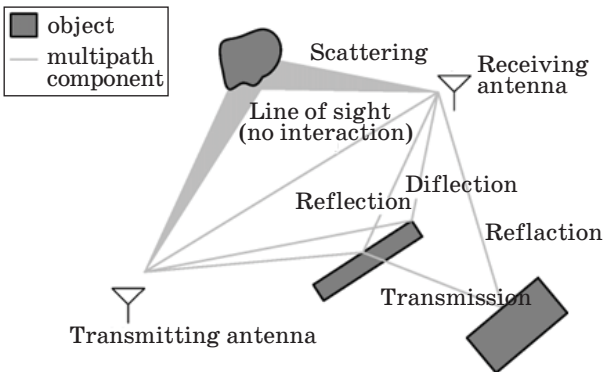

■ ***Fig. 1.*** Multipath phenomena in the land communication environments

tence of the both, LOS (Line-of-Sight) component and the NLOS component, known as Ricean fading described by the parameter of fading K, that is, it can generally described both NLOS (Rayleigh) and LOS + NLOS (Ricean) fading. According to corresponding descriptions and formulas that follow from the numerous statistical models, the Rician parameter of fading can defined as the ratio of the coherent and incoherent component of the signal intensity [16–30]

$$K = \frac{Intensity\_of\_LOS\_component}{Intensity\_of\_NLOS\_component} = \frac{I_{co}}{I_{inc}}. \quad (1)$$

The incoherent component actually describes the multiplicative noise inside communication channel. The main idea in the proposed framework is that we can use the K-factor to predict information data stream parameters both in MIMO correlated and uncorrelated antennas, such as capacity and spectral efficiency based on results obtained in [7–10, 31]. Therefore, the knowledge of factor K is necessary for analyze multipath communication channels capacity and spectral efficiency.

Multibeam antennas are usually used for achieving so-called spatial diversity introduced for improve the quality and reliability of a wireless link between arbitrary subscriber and base station (BS) or access point antenna. Usually in densely populated areas, there is no pure LOS between the transmitter and the receiver [7–10, 31]. As a result, multipath fading effect overlaps the information signal propagating along the transmitter-receiver path. In spatial diversity several receive and transmit antennas are placed at a distance from each other. Thus, if one antenna experiences a fade, another one will have an LOS or a pure information signal without noise. Figure 2 shows the basic principle of spatial diversity.

The same signal is fed through a single antenna or multiple antennas, and the same signal is captured by a single antenna or multiple antennas. In Fig. 2 several antennas are placed in a distance from each other. There are various obstacles on the signal's path. Despite the multipath fading effect that usually occur in other receivers, the desired receiver can get a fairly good signal.

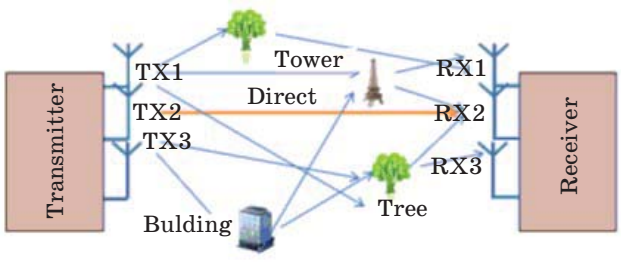

■ *Fig. 2.* Spatial diversity schematically presented

In an adaptive antenna system (AAS), multiple antennas are used both at the transmitting and receiving side of a communication link to adaptively optimize the transmission over the channel. An AAS can focus its transmitted energy towards the receiver, and while receiving, it can focus its energy towards the transmitter. The technique used in AAS is known as *beam forming* [7]. Figure 3 shows the basic principle of AAS.

Beam forming enables directional signal transmission or reception without manually steering the antennas. In the beam forming technique, several transmitters are set apart from each other (see details in [7] and the bibliography therein). They all transmit the same signal with different phase difference and delay. As a result, the interference that occurred in all the transmitters can be used to steer a signal to a specific direction.

When one antenna transmits a signal to the multiple receive antennas, the system is known as Single-output Multiple-input (MISO). Here one signal is transmitted and two or more are received. Receive diversity is used in the MISO antenna technique. In the SIMO (Single-input Multiple-output) antenna technique, multiple antennas are used at the transmitter while a single antenna is used at the receiver. It is a comparatively new technology [7]. This has been a favorite as only multiple antennas need to be installed in the BS. Transmit diversity technique, as a type of controlled diversity technique, which provides spatial repetition of transmitted signals through different antennas, is used in the case of MISO.

The MIMO transmission techniques and configurations were proposed to support radio access technologies, such as the WLAN, WiMAX and LTE standards [32–35]. MIMO is an effective technology based on spatial diversity surfacing from the usage of multiple antennas at both terminal ends of communication network to improve its reliability, increase spectral efficiency and achieving spatial separation of users for multi-user interference (MUI) elimination. Spatial diversity is also beneficial for multiple user (MU) cellular systems where spatial resources can be used to transmit information data to multiple users simultaneously [30–35].

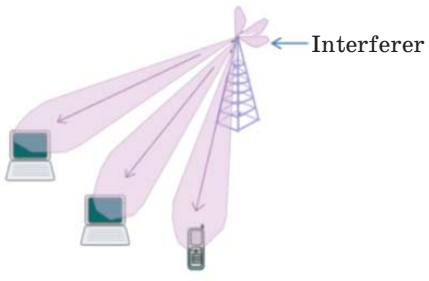

■ *Fig. 3.* Adaptive antenna system schematically presented

The MU-MIMO was performed as a set of advanced MIMO techniques. This advanced technology exploits the availability of multiple independent user equipment's (UEs) in order to enhance the communication capabilities of each individual UE (stationary or mobile). According to [34], the classical presentation of single user (SU) MIMO network is shown in Fig. 4, *a*, as a comparison with that for MU-MIMO network (Fig. 4, *b*).

It is clearly seen that for each mobile subscriber (MS) in downlink communication, the BS, as a multiple output antenna system send for each user with number i the corresponding data via the corresponding propagation channel with its response, caused by multipath fading occurring in real communication environment that, finally, corrupt information data passing via each channel with noise.

In MIMO system, presented by expression (2), the corresponding weight matrix $\mathbf{W}^{\mathrm{T}}$ forms relations between output signals' voltage, V_m, and those for the inputs, U_n, of a $M \times N$ planar array of the beam former at the both terminal, the BS and the MS (Fig. 5):

$$\mathbf{U} = \mathbf{W}^{\mathrm{T}}\mathbf{V}, \det \mathbf{W} \neq 0, \qquad (2)$$

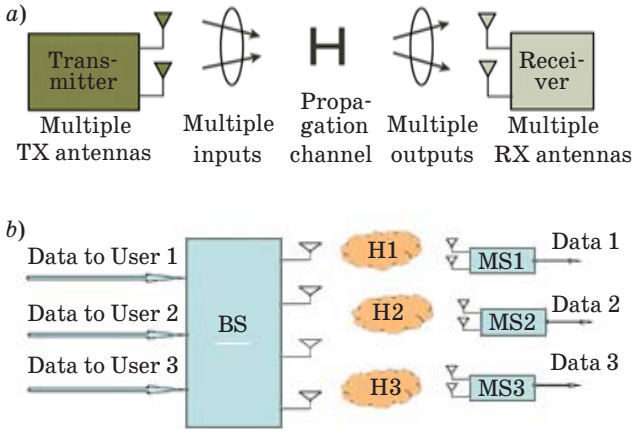

■ ***Fig. 4.*** SU-MIMO (*a*) and MU-MIMO (*b*) network, extracted from [34]

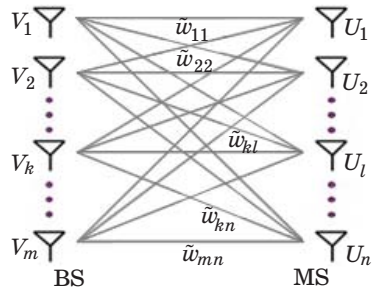

■ ***Fig. 5.*** MU-MIMO network

where

$$\mathbf{W} = \begin{bmatrix} \tilde{w}_{11} & \cdots & \tilde{w}_{1n} \\ \vdots & & \vdots \\ \tilde{w}_{m1} & \cdots & \tilde{w}_{mn} \end{bmatrix} \qquad (3)$$

is the weight matrix.

For SIMO or MISO variants the above 2D matrix deduces into 1D case:

$$\mathbf{U} = \mathbf{W}^{\mathrm{T}}\mathbf{V} = [\tilde{w}_1 \ldots \tilde{w}_m]\mathbf{V}, \qquad (4)$$

where $\tilde{w}_m = NSR$ defines multiplicative noise to signal ratio [7].

Capacity and Spectral Efficiency of the Channel

Next important task of the problem is the knowledge of the capacity or a spectral efficiency that *a-priory* allows estimating an operator's cost structure for a given service and grade of service that determines by:

— required amount of frequency spectrum;

— required number of BS or users' access points;

— required number of sites and associated site maintenance, and

— ultimately, consumer pricing and affordability.

Finally the increase of spectral efficiency will leads to:

— improved operator costs;

— reduced equipment per subscriber;

— reduced numbers of sites in capacity limited areas;

— reduced barriers to new operators;

— better use of available spectrum;

— especially important for limited mobility spectrum;

— improved end-user affordability, especially for broadband services.

These deployment parameters of MIMO system arrangement in terrestrial areas of service will give the following advantages for designers of such system, that is,

— as subscriber penetration increases;

— as per-user data rates increase;

— as quality of service (esp. data) requirements increase.

Increase of each channel capacity (or maximum data rate) means faster response times and higher speeds, a larger amount of users that can be able to transfer more data simultaneously and at higher speeds.

In our further description of the matter, we will get the *K*-factor from the measurements described in [7, 10–16] for various terrestrial built-up environments. The knowledge of *K*-factor allow us to predict the capacity and spectral efficiency of each separate channel of the multi-beam MIMO system caused by fading phenomena, which is individual

for each subscriber, located in areas of service, as well as the probability of Bit Error Rate (BER) of the information data stream inside each subscriber channel.

Then, we will analyze a key question: if using the proposed stochastic multi-parametric model for the MIMO system based on adaptive multi-beam antennas, we can increase the system capacity and will allow to designers of wireless networks to obtain maximal data rates, better channel conditions and, as a result, much better service and transmission performances [7–10, 31].

Modeling of *K*-factor in Built-up Environments

As was shown in [6, 7, 11–14], the fade parameters K_i for each beam-channel of individual antenna element reversely proportional to weight parameters of each antenna element $\tilde{w}_i$, that is, $\tilde{w}_m \sim K_m^{-1}$. If so, we can, using information of the *K*-parameter of fading occurring in each specific urban and sub-urban environment, investigate the capacity and spectral efficiency of each user individual channel.

K-factor in space domain. The main goal of usage of multi-beam antennas was to deploy in existing and advanced communication networks so-called spatial filtering of each desired signal. Usage of multiple beams concept with narrow beam width allows eliminating the inter-user interference, minimizing the multiplicative noise caused by fading phenomena occurring in the multipath communication channels, mostly for urban and sub-urban environments, and finally, tracking each MS during his existence in area of service of multi-beam BS antenna.

In each direction in azimuth and elevation domains for a current position of the desired subscriber the channel specific response should be introduced, and it was proposed to define this response by Ricean *K*-parameter of fading, as a ratio of the coherent (e.g. signal) and incoherent (e.g. noisy) components of the recorded signal. This parameter was evaluated in [7, 11–14] for different terrestrial scenarios, rural, mixed residential, sub-urban and urban, and was shown that this parameter fully depends on features of built-up terrain, such as buildings' density, overlay profile, orientation and elevation with respect to BS and MS antenna, and heights of the terminal antennas. The expression for *K*-factor along the radio path *d* between two terminal antennas can be given as [7]:

$$K = \frac{I_{co}}{I_{inc}} = \frac{\exp\left\{-\gamma_0 d \dfrac{\bar{h} - z_1}{z_2 - z_1}\right\}}{\dfrac{\Gamma}{8\pi} \cdot \dfrac{\lambda l_h}{\lambda^2 + \left[2\pi l_h \gamma_0\right]^2} \cdot \dfrac{\lambda l_v}{\lambda^2 + \left[2\pi l_v \gamma_0 \left(\bar{h} - z_1\right)\right]^2}} \times$$

$$\times \frac{\left[\dfrac{\sin\left(kz_1 z_2 / d\right)}{2\pi d}\right]^2}{\dfrac{\left[\left(\lambda d / 4\pi^3\right)^2 + \left(z_2 - \bar{h}\right)^2\right]^{1/2}}{d^3}}. \qquad (5)$$

For the urban and sub-urban environments following, we get according to [7]:

$$K = \frac{I_{co}}{I_{inc_1} + I_{inc_2}} = \exp\left\{-\gamma_0 d \frac{\left(z_1 - \bar{h}\right)}{\left(z_2 - z_1\right)}\right\} \times$$

$$\times \frac{\sin^2\left(kz_1 z_2 / d\right)}{4\pi^2 d^2} \Bigg/ \left(\frac{\Gamma \lambda l_v \left[\left(\lambda d / 4\pi^3\right) + \left(z_2 - \bar{h}\right)^2\right]^{1/2}}{8\pi \left[\lambda^2 + \left(2\pi l_v \gamma_0 \left(z_1 - \bar{h}\right)\right)^2\right] d^3} + \right.$$

$$\left. + \frac{\Gamma^2 \lambda^3 l_v^2 \left[\left(\lambda d / 4\pi^3\right) + \left(z_2 - \bar{h}\right)^2\right]}{24\pi^2 \left[\lambda^2 + \left(2\pi l_v \gamma_0 \left(z_1 - \bar{h}\right)\right)^2\right]^2 d^3} \right). \qquad (6)$$

Here, in formulas (5), (6), $\gamma_0 = 2\bar{L}\upsilon/\pi$ is the density of the buildings' contours [in km^{-1}], υ is the density of buildings in the area of service [in km^{-2}], $\bar{L}$ is the average length (or width) of buildings [in m], depending on its orientation with respect to terminal antenna, Γ is the absolute value of the reflection coefficient, l_v and l_h are the vertical and horizontal scales of coherency of the reflections from building walls, respectively [in m], $\bar{h}$ is the average buildings' height [in m], z_1 and z_2 are the heights of the MS and BS antenna, respectively.

We now present results of the numerical experiment carried out for one of the urban environment, the Ramat Gan market area in Israel (Fig. 6).

The BS antenna height was z_2 = 50 m. The outdoor desired MSs were located on the ground at the height of z_{1i} = 2 m. The simulations were performed for the following parameters of propagation: $\bar{h}$ = 25 m, γ_0 = 10 km^{-1}, l_v = 1÷2 m.

Results of simulation of *K*-parameter of fading is shown in Figs. 7, *a* and *b* for the carrier frequency of *f*=1.800 and 2.400 GHz respectively.

Based on these results, we can now for each MS with number *i* estimate signal to multiplicative noise ratio via *K*-factor that determines the losses and fading effects in each noisy communication channel for each desired UE. This procedure allows obtaining the channel spectral efficiency as function of *K* for various configurations of MIMO system consisting *M* outputs and *N* inputs.

K-factor in the joint space-azimuth domain. The corresponding expressions for evaluation of *K*-parameter of fading, $K(r, \varphi)$, as function of the distance *r*, for the constant azimuth φ, or as a func-

tion of φ, for the constant r can be presented via power spectrum distribution in the joint r-domain and φ-domain. Thus, following the Ricean parameter of fading, described by formula (1) $K(r,\varphi)=\dfrac{I_{co}(r,\varphi)}{I_{inc}(r,\varphi)}$, as a function of the distance r along the radio path between Tx and Rx and the azimuth φ of the antenna beam, can be presented via the average signal power spectrum in the space (along the radio path) and azimuth domains in the following form according to [7, 11–17]:

$$W(r,\varphi)=\langle I_{co}(r)\rangle\delta(\varphi-\varphi_0)+ +\langle I_1(r)\rangle f_1(r,\varphi)+\langle I_2(r)\rangle f_2(r,\varphi), \quad (7)$$

where $\delta(\varphi-\varphi_0)=1$ for $\varphi=\varphi_0$ (i.e., in the direction of the direct visibility from the Tx to the Rx); $\delta=0$ otherwise. The expression in (7) consists of three main terms, the coherent component (the first summand) and the incoherent component of the total power spectrum, consisting two terms (second and third summand), that is,

$$\langle I_{co}(\mathbf{r})\rangle=\exp\left\{-\gamma_0 r\frac{F(z_1,z_2)}{(z_2-z_1)}\right\}\frac{\sin^2(kz_1z_2/r)}{4\pi^2r^2}; \quad (8a)$$

$$\langle I_1(\mathbf{r})\rangle=\left[1+(1+\xi)^2\frac{1+\left(kl_v\gamma_0\bar{h}\right)^2}{1+\left(l_v\gamma_0\xi\left(\bar{h}-z_1\right)\right)^2}\right]\times \times\frac{(\gamma_0 r)^2(1-\xi)\exp[-\gamma_0 r(1-\xi)]}{(2+\gamma_0 r)}\frac{(1-a(r))}{\sqrt{1-a^2(r)}}; \quad (8b)$$

$$\langle I_2(\mathbf{r})\rangle=\xi\frac{\sqrt{1-b^2(r)}-\sqrt{1-2b^2(r)}}{b(r)}. \quad (8c)$$

The expression in (7) consists also of two main terms; f_1 and f_2, that can be presented as:

$$f_1(\varphi)=\frac{2z_1^2(\gamma_0 r)^2}{(z_2+\bar{h})}\frac{\varsigma'(1-\cos\varphi)}{\bar{h}}\frac{\exp[-A(\varphi)]}{B(\varphi)}; \quad (9a)$$

$$f_2(\varphi)=\frac{2\bar{h}(\gamma_0 r)}{(z_2+\bar{h})}\left[1+\left(\frac{\bar{h}}{z_2}\right)\frac{1+(kl_v\gamma_0 r)^2}{1+(\gamma_0\varsigma' r)^2}\right]\times \times\frac{\exp[-A(\varphi)]}{B(\varphi)}. \quad (9b)$$

Here

$$A(\varphi)=\gamma_0 r\left(\frac{\bar{h}}{z_2}+\frac{\varsigma'}{2}\frac{(1+\cos\varphi)}{\left[1+\dfrac{\gamma_0 r}{2}\left(1+\dfrac{\bar{h}}{z_2}\right)(1-\cos\varphi)\right]}\right) \quad (10a)$$

and

$$B(\varphi)=\left[1+\frac{\gamma_0 r}{2}\left(1+\frac{\bar{h}}{z_2}\right)(1-\cos\varphi)\right], \quad (10b)$$

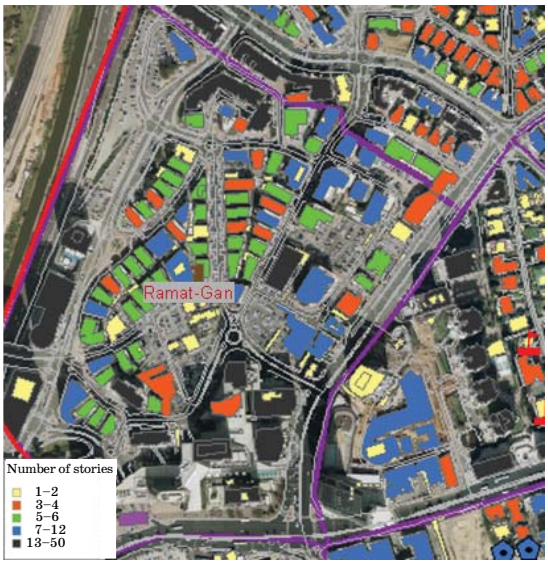

■ ***Fig. 6.*** Ramat Gan Built-up area; number of building floors are indicated by the corresponding color

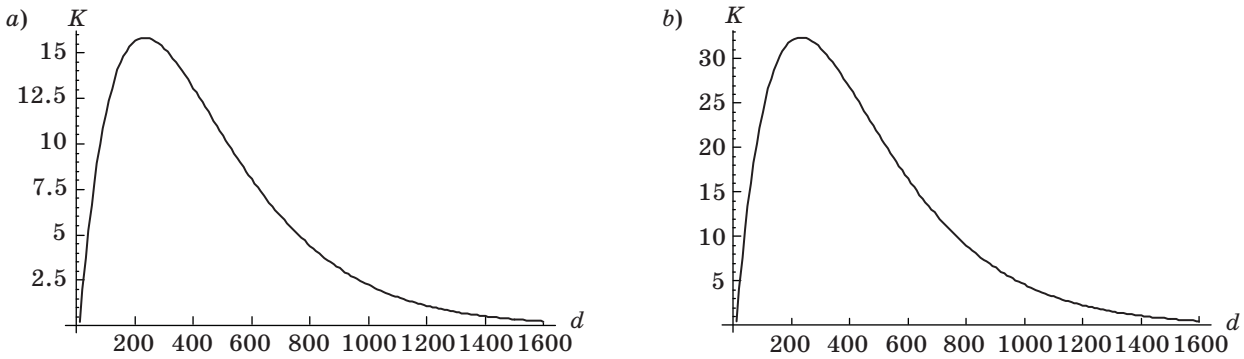

■ ***Fig. 7.*** The K-factor vs. distance between BS and different MSs in Ramat-Gan market area for f = 1.8 GHz (*a*) and f = 2.4 GHz (*b*)

where $\varsigma' = \frac{\left[\left(\lambda r / 4\pi^3\right) + \left(z_2 - \bar{h}\right)^2\right]^{1/2}}{z_2}$; $\xi = \frac{\left(z_2 - \bar{h}\right)}{z_2 - z_1}$;

$$a(r) = \frac{(2+\gamma_0 r)(1+\xi)}{1+(2+\gamma_0 r)(1+\xi)};\ b(r) = \frac{\pi^2}{(\pi+1)(\gamma_0 r)^{3/2}}.$$

In the above formulas, the function of the built-up terrain, $F(z_1, z_2)$, for the regularly and linearly distributed heights of buildings from $h_{\min}$ to $h_{\max}$ (i.e., for $n = 1$), having the mean height of $\bar{h} = \frac{h_{\min} + h_{\max}}{2}$, equals: $F(z_1, z_2) \approx \left(\bar{h} - z_1\right)$ [7, 11–17]; as above, $\gamma_0 = \frac{2\bar{L}v}{\pi}$; l_v is the vertical scale of correlation of the walls' roughness in the vertical plane; $\bar{L}$ is the average building's length (or width, depending of its orientation to the antenna beam); v is the number of buildings per square kilometer; z_2 and z_1 are the heights of the BS and MS antenna heights, respectively, where always $z_1 < z_2$.

Finally, we can get for a Ricean K-factor:

$$K(r,\varphi) = \frac{\left\langle I_{co}(r)\right\rangle \delta(\varphi - \varphi_0)}{\left\langle I_1(r)\right\rangle f_1(r,\varphi) + \left\langle I_2(r)\right\rangle f_2(r,\varphi)}. \qquad (11)$$

It is important to analyze effects of two terms in the denominator, consisting functions of $\langle I_1(r)\rangle f_1(r, \varphi)$ and $\langle I_2(r)\rangle f_2(r, \varphi)$. Each of them relates to a different propagation phenomenon. The term $\langle I_1(r)\rangle f_1(r, \varphi)$ is the significant term that describes the influence of the scattering area located at the proximity of Rx. The term $\langle I_2(r)\rangle f_2(r, \varphi)$ describes the general effect of rare scatterers that are distributed uniformly in areas surrounding the Tx and MS. The influence of different scatterers for the three typical cases, depending on the BS antenna height.

Thus, when both antennas are lower than the height of the buildings, the both components, $\langle I_1(r)\rangle f_1(r, \varphi)$ and $\langle I_2(r)\rangle f_2(r, \varphi)$, should be taken into account. From formulas (9a) and (9b), as well as from (10a) and (10b), it follows that, if the BS antenna height increases up to $z_2 = \bar{h}$ then $\varsigma = \sqrt{\left(\lambda d / 4\pi^3\right)} \Big/ z_2 \ll 1$, $\left\langle I_2(r)\right\rangle f_2(r,\varphi)_{z_2 = h} \gg \left\langle I_1(r)\right\rangle f_1(\varphi)_{z_2 = h}$.

In the case of $\langle I_1(r)\rangle f_1(\varphi)$ is close to zero, and it means that all scatterers located in the far zone from the MS, near the BS, will influence the spreading of the total signal at the BS. With an increase in the height of the BS antenna, that is, $z_2 > \bar{h}$, the influence of buildings surrounding the MS on the total signal distribution will be more significant, and the term $\langle I_1(r)\rangle f_1(r, \varphi)$ becomes larger than the term $\langle I_2(r)\rangle f_2(r, \varphi)$, describing the effect of scatterers located close to the MS.

When the BS antenna is above the rooftop level the K-factor distribution in the azimuth domain $K(\varphi)$ [for the distance r being the constant] depends only on position and the distribution of scatterers (obstructions) close to MS. Influence of scatterers (buildings) in the proximity of MS on the signal received at the MS is increased and it contributes more than the scatterers surrounding the BS and then those located far from the MS.

Modeling of Capacity of MIMO Systems in Built-up Environments

Using now information of the K-parameter of fading occurring in each specific urban and suburban environment, one can investigate the capacity and spectral efficiency of each beam channel for each individual user. This situation is depicted in Fig. 8, by the $N \times M$ arrays representing a common set of scatterers inside the communication channel.

The break-through in the interest in MIMO channels [7–9, 31] came when it was realized that it gives a much higher throughput in the link when having many channels of lower gain than one channel with a high gain. The statement follows directly from Shannon's law for one channel in noise. The capacity grows linearly with the known and the unknown channel bandwidth B_w, and, in the particular case ($M = N = 1$), can be presented as:

$$C = B_w \log_2\left(1 + \frac{P}{B_w N_0}\right) \text{[bps]}, \qquad (12)$$

where $P/B_w N_0$ is the ratio of power signal to white noise, N_0 is the spectral density of white Gaussian noise, B_w is its waveband of white noise. When channels are independent their capacities may be added, so for M and N larger than 1, and $M > N$ we get:

$$C_{uncorr} = B_w N \log_2\left(1 + \frac{MP}{NB_w N_0}\right) \text{[bps]}. \qquad (13)$$

We can explain this formula in the following way: the power is divided equally between the N channels, since they have the same gain. Since the capacities of the channels are the same, we get a factor of N outside the log-function. The capacity (or spectral efficiency $\tilde{C} = C/B_w$) is almost constant

■ *Fig. 8*. MIMO antenna system

due to the high diversity order of MN. For the correlated case, we have only one channel, now with mean gain MN [7–9]:

$$C_{corr} = B_w \log_2\left(1+\frac{MNP}{B_w N_0}\right) \text{ [bps]}. \qquad (14)$$

Let us now analyze equations (13), (14) for various situations in the urban scene following to the approach proposed in [7, 26] where multiplicative noise was taken into account. Thus, taking into account multiplicative noise influence with effective power density N_{mul} as one of the Gaussian-like noise we can rewrite (12) as:

$$C = B_\omega \log_2\left[1+\frac{S}{N_0 B_\omega + N_{mul} B_\Omega}\right], \qquad (15)$$

where B_Ω is the frequency bandwidth of the multiplicative noise.

We should mention here, following [25, 26], that this procedure of replacing of equation (12) by equation (15) can only be done because of the similarity between the Ricean distribution and the Gaussian distribution for $K > 1$, and the fact that as the Ricean K parameter grows, the Ricean distribution approaches the Gaussian distribution in the limit. Using the approximate formula in equation (8) for the capacity (or for the spectral efficiency of the channel, $\tilde{C} = C/B_w$), we can now simplify the expressions obtained below for capacity, spectral efficiency ad BER, which are usually used in wireless communications [7, 25–35]. Again, equation (8) is valid when the LOS component of the total signal inside a channel exceeds the NLOS component, that is, when the K-factor is greater than a unit [7, 26].

This approach is similar to that proposed by Rappaport [1] analyzing MUI. Using the same procedure, as above, for multiple access networks, it was proved in [1] that the effects of MUI can be regarded as another source of effective noise, which raises the noise level for calculating the error rates. In this case we must introduce in formula (15) N_{add} together with the noise caused by MUI N_{int}. Furthermore, the above simple approach can be successfully used in cases of dynamic communication channels with fading, flat or multiplicative, where an additional source of noise, called multiplicative noise, must be taken into account [7, 26].

Above mentioned allows us to rewrite the Shannon's formula (15) accounting for the presence of multiplicative noise as

$$\tilde{C} = \log_2\left(1+\frac{P}{N_{add}+N_{mul}}\right) = \log_2\left(1+\left(\frac{N_{add}}{P}+\frac{N_{mul}}{P}\right)^{-1}\right). \qquad (16)$$

Using the above introduced notations, we finally get the capacity as a function ofthe K-factor and the additive noise:

$$\tilde{C} = \log_2\left(1+\left(\frac{N_{add}}{P}+K^{-1}\right)^{-1}\right) = \log_2\left(1+\frac{K\dfrac{P}{N_{add}}}{K+\dfrac{P}{N_{add}}}\right), \qquad (17)$$

where, as above, $\dfrac{S}{N_{mult}} = \dfrac{I_{co}}{I_{inc}}$, and we use here the definition of K as: $K_m = \dfrac{I_{co}}{I_{inc}}$.

If so, according to [7–10], we can obtain for correlated and uncorrelated elements of the multi-beam antenna the following formulas for spectral efficiency of the (M/N)-element antenna system:

— for correlated multi-beam antenna elements

$$\tilde{C}_{corr} = \log_2\left(\frac{1+MN\left(K_m\left(\dfrac{P_m}{N}\right)_{add}\right)}{\left(K_m+\left(\dfrac{P_m}{N}\right)_{add}\right)}\right) \text{ [b/s/Hz]}; \qquad (18a)$$

— for uncorrelated multi-beam antenna elements

$$\tilde{C}_{uncorr} = N\log_2\left(\frac{\left(K_m\left(\dfrac{P_m}{N}\right)_{add}\right)}{\left(K_m+\left(\dfrac{P_m}{N}\right)_{add}\right)}\right) \text{ [b/s/Hz]}. \qquad (18b)$$

Here, $(P_m/N)_{add}$ is the signal to additive Gaussian noise ratio, which usually is taken into account in the literature. We also accounted the multiplicative noise caused by fading multipath phenomena occurring in each m channel.

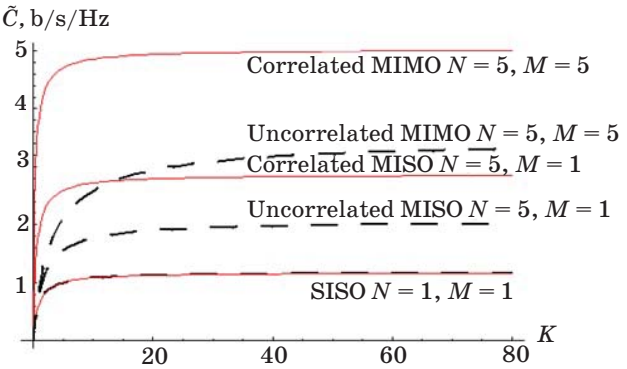

■ ***Fig. 9.*** Spectral efficiency of the MIMO and MISO systems vs. K-factor; as an example, SISO system is also presented

In both cases, the spectral efficiency depends not only on the number of output and input antenna elements, but also on the *K*-factor of fading. This dependence for different configurations of MIMO system is presented in Fig. 9.

It is clear seen that correlated antenna elements allow achieving better spectral efficiency compared with that for uncorrelated antenna elements.

Numerical Analysis of Capacity and Weight Coefficients for MIMO System

The following scheme (Fig. 10) will explain location and angles of the antennas in our numerical experiment. *LOS*: φ_0=0, φ=180°.

Base station located at $r = 0$ (see Fig. 10). When $\varphi_0 = 0$ it means that the direction of the beam is parallel to the ground, and is directed to the receiving antenna at distance *r*. For the best signal, receiving antenna should be rotated horizontally at an angle of $\varphi = 180°$, directly to the transmitting antenna. The initial parameters we take for an urban environment shown in Fig. 6 are the following: $\upsilon = 0.0001$ m^{-2}; $L = 100$ m; $l_\upsilon = 2$ m; $l_h = 1$ m; $h = 40$ m; $z_1 = 2$ m; $z_2 = 5$ m; $f = 900$ MHz.

The 1D dependence W(r) in space domain. This is a plot of *weight coefficients W*, defined by (2) to (4) for adaptive terminal antennas, as a function of the distance *r* between the BS and MU antennas (Fig. 11).

As it is seen from Fig. 11, at the close ranges from the BS antenna a tendency of decrease of coefficient *W* can be explained by effects of increase the LOS component and decrease of multipath effect on the weight coefficients, because With increase of distance between two terminal antennas, BS and MU, effects of multiple scattering from obstructions, natural and man-made, becomes prevailed on LOS, that is, the LOS component decreases, but multipath NLOS component increases with movements of subscribers far from the transmitter.

The 1D dependence W(φ) in the azimuth domain. The same tendency is observed for the weight coefficients in the azimuth domain (Fig. 12). As it is seen from Fig. 12, when BS and MU antennas are directly opposite to each other, we have maximum LOS component, that is, minimum of the parameter *W*. This tendency is decreased with increase of the distance between BS and MU antennas, because the multipath phenomena caused by multiple scattering from obstructions surrounding both terminal antennas becomes prevail against "pure" propagation phenomena. The same is observed with increase of azimuth angle between BS and MU from the LOS direction (when $\varphi = 180°$, see Fig. 12).

3D dependence of W(φ, r) in the joint distance-azimuth domain. Now we present a 3D-plot of weight coefficients *W* versus φ and *r* (Fig. 13). The presented here results are generalize all those shown above shown by Figs. 11, 12. Here a 3D-plot of weight coefficients *W* is presented in the joint φ-*r* domain for different azimuth angles of adaptive antenna beam and for various distances between BS and MU antenna. The right column presents the weight coefficient *W* versus *r* and φ.

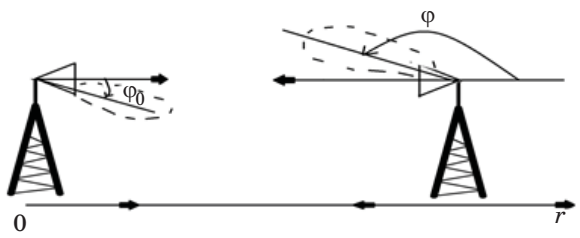

■ ***Fig. 10***. Scketched geometry of numerical experiment with adaptive antennas

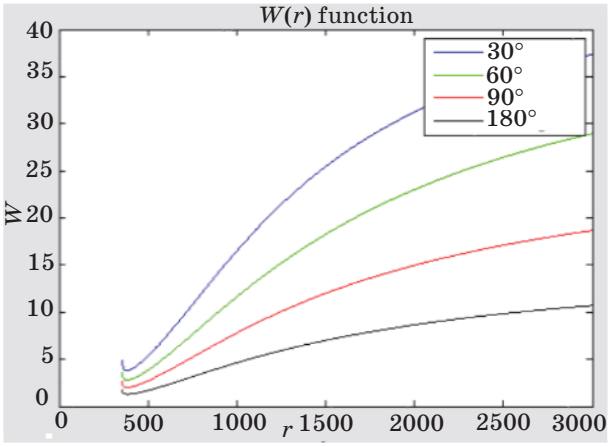

■ ***Fig. 11***. Weight coefficients *W* of the adaptive antenna, vs. distance *r* for 4 various azimuth angles φ

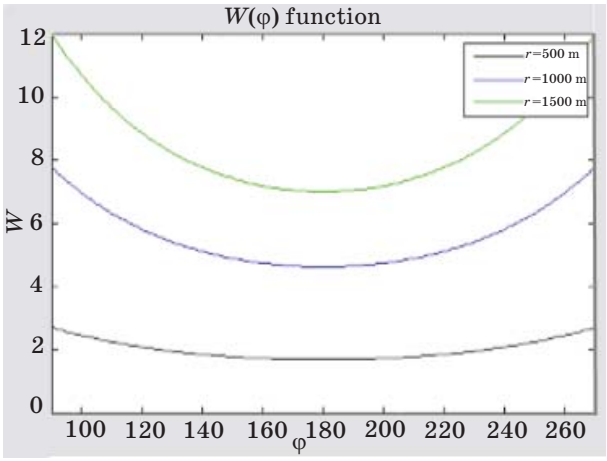

■ ***Fig. 12***. Weight coefficients distribution in the azimuth domain for the distance *r* from the transmitter

As it is seen again, the minimum of noise-to-signal ratio, that is of weight coefficients, W, is obtained when two antennas in LOS conditions one opposite the second (i.e., $\varphi = 180^{o}$). With increase of distances, this effect becomes weaker and the corresponding dependence becomes smoother.

The 1D dependence C_{uncorr} (r) in space domain for uncorrelated-element antenna. In Fig. 14 a plot of C_{uncorr} as a function of distance r is shown for different azimuth of the antenna inclination (see Fig. 10).

The upper three curves represent MIMO 8×8 settings and the lower three curves represent SISO (1×1) for simple comparison between antenna system arrangements. The behavior of the curves in Fig 14 is similar to those shown in Fig. 11 because C_{uncorr} depends on K and acts the same way as seen from the formula (18b).

The 1D dependence C_{corr} in space domain for correlated-element antenna. In Fig. 15 a plot of C_{corr}, as a function of r.

As it is seen, there is no any sufficient difference in arrangement of MIMO antenna system, correlated and uncorrelated; only the spectral efficiency is slightly better in the case of correlated antennas. The distance and azimuth effects are similar.

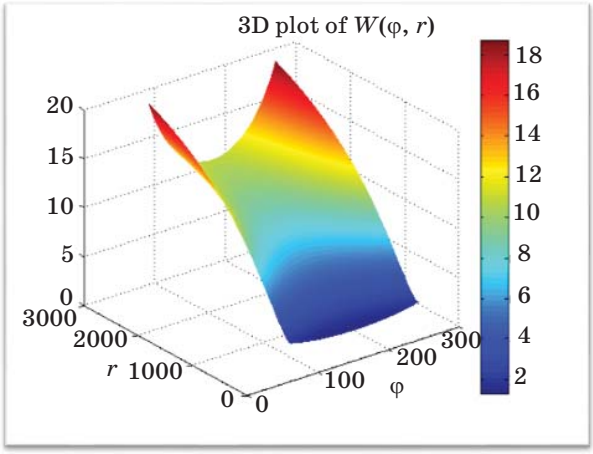

■ ***Fig. 13.*** 3D-plot of W as a function or φ and r

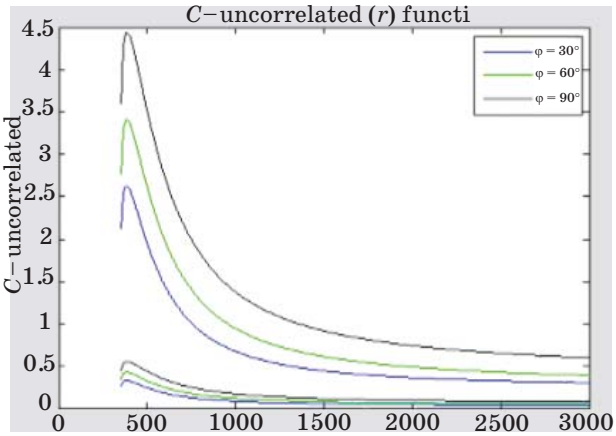

■ ***Fig. 14.*** C_{uncorr} vs. distance r for various azimuth angles φ

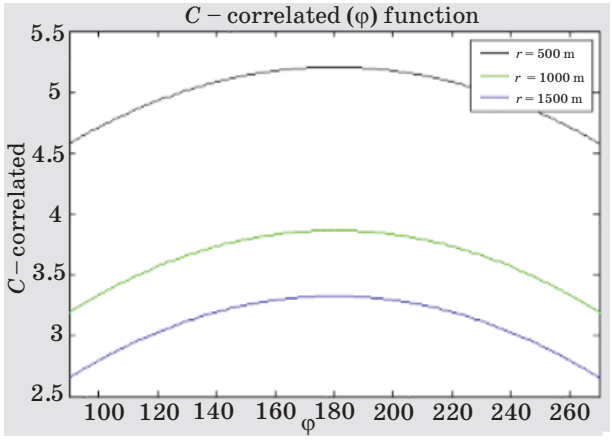

■ ***Fig. 15.*** C_{corr} vs. distance r for various azimuth angles φ

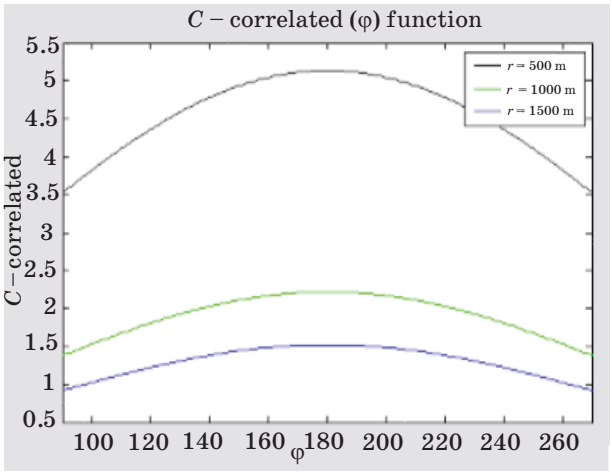

■ ***Fig. 16.*** C_{uncorr} vs. the azimuth angle for the distance r

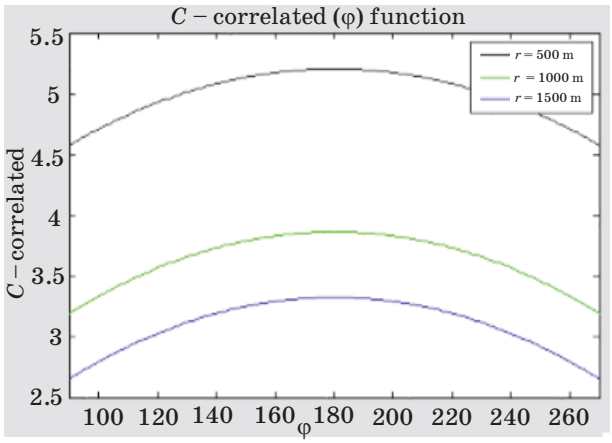

■ ***Fig. 17.*** C_{corr} vs. the azimuth angle for the distance r

1D dependence of C_{uncorr} (φ) in azimuth domain. In Fig. 16 a plot of C_{uncorr}, as a function of φ for the distance r=500, 1000, 1500 m, is shown.

As it is seen, there is no any sufficient difference in arrangement of MIMO antenna system, correlated and uncorrelated; only dependence on K slightly better in the case of correlated antennas. The distance and azimuth effects are similar.

The 1D dependence of C_{corr} (φ) in azimuth domain. In Fig. 17 a plot of C_{corr}, as a function of φ is shown for different distances between the transmitter and receiver antenna r = 500, 1000 and 1500 m.

The behavior of the graph in Fig. 17 is like in Fig. 12, because, according to formula (18a), C_{corr} depends on K (K=1/W) and acts at the same way as it is seen in Fig. 12, calculated for weight coefficients W.

Summary

Splitting the antenna up into several antenna elements with a possibility of adaptively combining the signals gives the well-known diversity gain, under the assumption of small correlation between the elements. The correlation depends on both the element pattern and the power distribution of the environmental spread. The diversity gain may be used on both the receiving and the transmitting side, but the highest gain is achieved when both sides are being optimized jointly. The gain is not only maximized, but there is also a diversity order of order $M \times N$. The real benefit comes from realizing that there are a potentially large number of parallel channels with almost the same good properties. This benefit may also be realized through space-time-coding or feed-back from the receiver to the transmitter (see [34]).

References

1. **Rappaport T. S.** *Wireless Communications Principles and Practice*. New York, Prentice Hall, 1996. 641 p.
2. **Lee W. C. Y.** *Mobile Cellular Telecommunications Systems*. New York, McGraw Hill, 1989. 449 p.
3. *Mobile Radio Communications*. Ed by R. Steele and L. Hanzo. Cichester, John Wiley, 1999. 1090 p.
4. **Saunders S. R.** *Antennas and Propagation for Wireless Communication Systems*. New York, John Wiley & Sons, 1999. 426 p.
5. **Proakis J. G.** *Digital Communication*. New York, McGraw Hill, 2001. 1024 p.
6. **Blaunstein N.** *Wireless Communication Systems*. In: *Handbook of Engineering Electromagnetics*. Ed. by R. Bansal. New York, Marcell Dekkel, 2005. Pp. 417–481.
7. **Blaunstein N., and Ch. Christodoulou.** *Radio Propagation and Adaptive Antennas for Wireless Communication Links: Terrestrial, Atmospheric and Ionospheric*. 1st ed. New York, Taylor and France, 2007. 614 p.
8. **Andersen J. Bach.** Role of Antennas and Propagation for the Wireless Systems Beyond 2000. *Wireless Personal Communicat*., 2001, vol. 17, pp. 303–310.
9. **Andersen J. Bach.** Antenna Arrays in Mobile Communications: Gain, Diversity, and Channel Capacity. *IEEE Antennas and Propagation Magazine*, 2000, vol. 42, no. 2, pp. 12–16.
10. **Andersen J. Bach.** Array Gain and Capacity for Known Random Channels with Multiple Element Arrays at Both Ends. *IEEE Journal on Selected Areas in Communications*, 2000, vol. 18, no. 11, pp. 2172–2178.
11. **Blaunstein N.** Prediction of Cellular Characteristics for Various Urban Environments. *IEEE Antenna Propagation Magazine*, 1999, vol. 41, no. 6, pp. 135–145.
12. **Blaunstein N., Katz D., Censor D.,** et al. Prediction of Loss Characteristics in Built-up Areas with Various Buildings' Overlay Profiles. *IEEE Antenna Propagation Magazine*, 2001, vol. 43, no. 6, pp. 181–191.
13. **Blaunstein N., Kovacs I. Z., Ben-Shimol E.,** et al. Path Loss Prediction in Forested Environments. *Radio Sci*., 2002, vol. 37, pp. 396–406.
14. **Blaunstein N.** Distribution of Angle-of-Arrival and Delay from Array of Building Placed on Rough Terrain for Various Elevation of Base Station Antenna. *Journal of Communic. and Networks*, 2000, vol. 2, no. 4, pp. 305–316.
15. **Blaunstein N., Toulch M., Laurila J., Bonek E., Katz D.,** et al. Signal Power Distribution in the Azimuth, Elevation and Time Delay Domains in Urban Environments for Various Elevations of Base Station Antenna. *IEEE Trans. Antennas and Propagation*, 2006, vol. 54, no. 10, pp. 2902–2916.
16. **Tepedelenlioglu C., Abdi A., Giannakis G. B., and Kaveh M.** Estimation of Doppler Spread and Signal Strength in Mobile Communications with Applications to Handoff and Adaptive Transmission. *Wireless Commun. Mob. Comput*., 2001, vol. 1, pp. 221–242.
17. **Blaunstein N., Yarkoni N., and Katz D.** Spatial and Temporal Distribution of the VHF/UHF Radio Waves in Built-up Land Communication Links. *IEEE Trans. Antenna Propagation*, 2006, vol. 54, no. 8, pp. 2345–2356.
18. *Propagation in Physical Radio Channel*. Available at: http://www.wica.intec.ugent.be/research/propagation/physical-radiochannel (accessed 30 December 2012).
19. *Multipath Propagation*. Available at: http://en.wikipedia.org/wiki/Multipath_propagation (accessed 30 November 2009).
20. *How does Reflection Affect Radio Waves*. Available at: http://www.qrg.northwestern.edu/projects/vss/docs/communications/2how-does-reflection-affect-radio-waves.html (accessed 30 November 2012).

21. *The Laws of the Physical World*. Available at: http://www.peoplephysics.com/physics-laws10.html (accessed 30 December 2002).
22. *Reflection*. Available at: http://www.acoustics.salford.ac.uk/feschools/waves/reflect.php (accessed 01 January 2011).
23. *Fresnel Zones*. Available at: http://www.4gon.co.uk/solutions/technical_fresnel_zones.php (accessed 01 January 2011).
24. *Wave Diffraction*. Available at: http://www.acoustics.salford.ac.uk/feschools/waves/diffract3.php (accessed 01 January 2011).
25. *Ripple Tank*. Available at: http://en.wikipedia.org/wiki/Ripple_tank (accessed 30 December 2011).
26. **Yarkoni N., and N. Blaunstein.** Capacity and Spectral Efficiency of MIMO Wireless Systems in Multipath Urban Environments with Fading. *Proc. of European Conf. on Antennas and Propagation*, EUCAP-2006, Nice, France, November 6–10, 2006. 6 p.
27. **Telatar I. E., and Tse D. N. C.** Capacity and Mutual Information of Wideband Multipath Fading Channels. *IEEE Trans. Information Theory*, 2000, vol. 46, no. 4, pp. 1384–1400.
28. **Goldsmith A. J., and Varaiya P. P.** Capacity of Fading Channels with Channels Side Information. *IEEE Trans. Information Theory*, 1997, vol. 43, no. 6, pp. 1986–1992.
29. **Winters J. H.** On the Capacity of Radio Communication Systems with Diversity in a Rayleigh Fading Environments. *IEEE Select. Areas in Communication*, 1987, vol. 5, pp. 871–878.
30. **Chizhic D., Foschini G. J., and Valenzuela R. A.** Capacities of Multi-element Transmit and Receive Antennas: Correlations and Keyholes. *Electronic Letters*, 2000, vol. 36, pp. 1099–1100.
31. **Molisch A. F., Steinbauer M., Toeltsch M.,** et al. Capacity of MIMO Systems Based on Measured Wireless Channels. *IEEE Select. Areas in Communic.*, 2002, vol. 20, no. 3, pp. 561–569.
32. **Alouini M.-S., Simon M. K., and Goldsmith A. J.** Average BER Performance of Single and Multi-Carrier DS-CSMA Systems over Generalized Fading Channels. *Wiley Journal on Wireless Systems and Mobile Computing*, 2001, vol. 1, no. 1, pp. 93–110.
33. **Goldsmith A. J.** The Capacity of Downlink Fading Channels with Variable Rate and Power. *IEEE Trans. on Vehicular Technol.*, 1997, vol. 46, no. 3, pp. 569–580.
34. **Blaunstein N., and Sergeev M. B.** Integration of Advanced LTE Technology and MIMO Net-work Based on Adaptive Multi-beam Antennas. *Lecture Notes in Computer Science (Including Subseries Lecture Notes in Artificial Intelligence and Lecture Notes in Bioinformatics),* 2012, vol. 7469 LNCS, pp. 164–173.
35. **Sudhir Babu A., and K. V. Sambasiva Rao.** Evaluation of BER for AWGN, Rayleigh and Rician Fading Channels under Various Modulation Schemes. *Int. Journal of Computer Applications*, July 2011, vol. 26, no. 9, pp. 23–28.